

# A Ray-Tracing Propagation Model for Digital Broadcast Systems in Urban Areas

Harry R. Anderson<sup>1</sup>, M.Sc., P.Eng.

EDX Engineering, Inc.

P.O. Box 1547

Eugene, Oregon 97440 U.S.A.

Tel: (503) 345-0019 Fax: (503) 345-8145

**Abstract**—This paper presents a propagation model for characterizing the channel response for digital systems in urban areas where multiple reflections from buildings are encountered. A deterministic ray-tracing propagation model was used to predict the time delay and fading characteristics for the channel in a hypothetical urban area. The analysis shows that due to multiple reflection and diffraction sources, the RMS delay spread of the channel in urban areas can be several hundred nanoseconds, indicating that very effective equalizers will be required to yield successful performance of high data rate digital systems such as 20 Mbit 16QAM digital HDTV. The channel response results presented here also suggest that polarization diversity may be a useful technique to mitigate some of the channel impairments predicted by the propagation model.

## I. INTRODUCTION

There currently is a migration from traditional analog radio and television broadcast systems to new digital systems which promise improved frequency response, increased information content, and improved immunity to noise. The coverage of analog broadcast systems has usually been predicted based on the median field strength available at a receive location, along with certain other time and location variability statistics to account for fading and prediction uncertainties. This is a simple and reasonably useful approach to system performance prediction, although some important channel impairments such as FM multipath distortion and TV ghosting can not be predicted with simple signal level models.

When compared to analog systems, digital systems are more sensitive to channel degradation in the form of multipath distortion and fading. Such impairments can result in data bits decoded in error. If the bit error rate (BER) is too large, correct decoding of some or all of a frame of data becomes impossible, resulting in a complete loss of the information content of the transmission. This is especially true in simple high data rate 16QAM systems such as digital HDTV where the transition from a low BER with an excellent picture to a high BER and a lost picture can occur with a change of only a few dB

in the average signal-to-noise ratio (SNR). This contrasts with analog systems in which the picture quality is gradually degraded as SNR decreases and multipath ghosting increases.

The picture quality effects as a function of SNR are well known to HDTV system designers, at least when the noise is additive white gaussian noise (AWGN). What has not been adequately studied is HDTV performance with realistic multipath environments where literally hundreds of symbol pulse echos may be presented to the receiver. A growing body of research with digital mobile communication systems shows that such multipath degradation is a more critical indicator of overall system performance in an urban area than is the SNR. Because some relevant features of the propagation environment may change with time (moving cars, airplanes, etc.), the channel response at any given location cannot always be considered as static, placing stringent demands on the performance of the long multi-tap adaptive equalizers currently planned for HDTV receivers.

Errors in digital systems due to multipath are sometimes referred to as "irreducible" in that increased transmitter power will not correct them as it will with errors due to AWGN. It is therefore inappropriate to assume that multipath errors, or inadequate equalizer performance, can be mitigated by increased transmitter power in the HDTV power budget equation.

For the research described in this paper, a model was developed which can simulate multipath propagation conditions in an urban environment. The model uses a ray-tracing approach based on geometric optics and the uniform theory of diffraction (UTD) to identify individual multipath signal contributions at the receiver. The model was used in conjunction with a hypothetical urban area in which block dimensions and street widths are similar to those found in a downtown urban area such as Manhattan. The time delay and amplitude of predicted multipath signals then reasonably resemble those that might be found in a real urban reception location.

Using this propagation model, the channel response throughout the urban area is described in terms of the signal level, RMS delay spread, and the fading statistics at each point in the service area. This information is devel-

<sup>1</sup>Part of this research was done while the author was resident at the Centre for Communications Research, University of Bristol, U.K.

oped for both horizontally-polarized (HP) and vertically-polarized (VP) transmissions.

## II. PROPAGATION MODEL

A general model of the low-pass impulse response for the urban transmission channel attributed to Turin[1], is:

$$h(t) = \sum_{n=1}^N A_n \delta(t - \tau_n) \exp(-j\theta_n) \quad (1)$$

in which the impulse response  $h(t)$  is the sum of a set of  $N$  impulses arriving at times  $\tau_n$  with amplitudes  $A_n$  and phases  $\theta_n$ .

To employ this model, it is necessary to identify the amplitudes, time delays and phases of the  $N$  constituent components of this response. The components may consist of the line-of-sight signal received from the transmitter, and a variety of signals received from reflecting surfaces, diffracting corners, and scattering surfaces. By using a technique known as ray-tracing, the energy emitted from the source transmitting antenna is geometrically traced to determine those surfaces or corners which are illuminated. Because ray-tracing inherently provides pulse delay or spreading information, it has become an attractive approach to propagation modelling for digital communication systems. Ray-tracing is a fundamental technique which has long been used for dealing with problems in geometric optics (GO) and high-frequency EM field and propagation problems [2]. Channel amplitude response statistics using ray-tracing are reported in [3]. More recent efforts using ray-tracing to predict both the amplitude and pulse spread channel response have been reported in a number of papers (for example, see [4], [5], and [6]).

For the ray-tracing model used here, each illuminated surface is replaced by an image transmitter or scattering source such that the radiation from the image represents (in amplitude, phase and radiating directions) the energy reflected from the source. Similarly, an illuminated corner is replaced by an equivalent wedge diffraction source. With this first set of images and illuminated corners in place, each of them is then considered in turn by ray-tracing to determine the surfaces and corners they illuminate. Energy from these second reflecting surfaces represent two reflection echos. This process is repeated for as many iterations as may be relevant to the problem at hand, or which are practical from a computational point of view. Ten orders of reflections, with several thousand resulting image sources and diffracting corners, are possible. The ray-tracing model used here incorporates a novel geometric decimation of the propagation environment to identify relevant reflecting surfaces and diffracting corners. This technique allows for a computationally efficient implementation of ray-tracing on PC-type platforms. This model also handles arbitrary wall and corner

geometry (in two dimensions) so that systematic one-to-one mapping from the real propagation environment to the model propagation environment is possible.

Reflection and diffraction are two of five propagation primitives incorporated in the model, which include:

1. Free space transmission
2. Reflection
3. Diffraction
4. Diffuse wall scattering
5. Wall transmission

These fundamental propagation primitives are used in appropriate combinations according to the ray path geometry to form an ensemble of interactions with the propagation environment which ultimately yield the amplitude and phase of the ray arriving at the receiver. The particular calculation details for each of the five propagation primitives are presented below.

### A. FREE SPACE TRANSMISSION

Free space transmission occurs in a uniform vacuum where no elements of the propagation environment (walls, corners, ground) are encountered. The formula for received power can be found in numerous references (for example, [7]), and is usually given with transmit and receive antenna gains, as follows:

$$P_r = \frac{P_t G_t G_r \lambda^2}{(4\pi)^2 d^2} \quad (1)$$

where  $P_r$  is the power received at the terminals of the receive antenna,  $P_t$  is the transmitter power delivered to the terminals of the transmit antenna,  $G_t$  and  $G_r$  are the transmit and receive antenna gains, respectively, in the relevant ray departure and arrival directions,  $\lambda$  is the wavelength, and  $d$  is the path distance from transmitter to receiver. As shown below, when the ray from the transmitter to receiver interacts with the propagation environment, the received power level for that ray as calculated in (1) is reduced by the appropriate reflection, diffraction, diffuse scattering, or wall transmission coefficients.

### B. REFLECTION

The amplitude and phase of the reflected energy is determined by the reflection coefficient. The reflection coefficient depends on the angle of incidence (illumination), the conductivity, permittivity, and roughness of the reflecting surface, and the polarization of the incident wave. For plane wave incidence, the general reflection coefficient  $R$ , is

$$R = R_s \cdot \rho$$

where  $R_s$  is the smooth surface reflection coefficient and  $\rho$  is the surface roughness attenuation factor (a scalar).

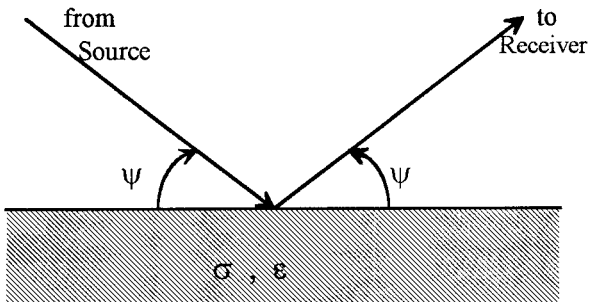


Figure 1: Reflection geometry.

For parallel and perpendicular polarizations, respectively, the smooth surface reflection coefficients are

$$R_{s\parallel} = \frac{\sin \psi - \sqrt{\epsilon - \cos^2 \psi}}{\sin \psi + \sqrt{\epsilon - \cos^2 \psi}} \quad (3)$$

$$R_{s\perp} = \frac{\epsilon \sin \psi - \sqrt{\epsilon - \cos^2 \psi}}{\epsilon \sin \psi + \sqrt{\epsilon - \cos^2 \psi}} \quad (4)$$

where  $\psi$  is the angle of incidence and  $\epsilon$  is the complex permittivity given by

$$\epsilon = \epsilon_r - j60\sigma\lambda$$

where  $\epsilon_r$  is the relative dielectric constant of the reflecting surface,  $\sigma$  is the conductivity of the reflecting surface in Siemens/m, and  $\lambda$  is the wavelength of the incident radiation.

The roughness attenuation factor  $\rho$  is given in [8] as

$$\rho^2 = e^{-2\delta} \quad (5)$$

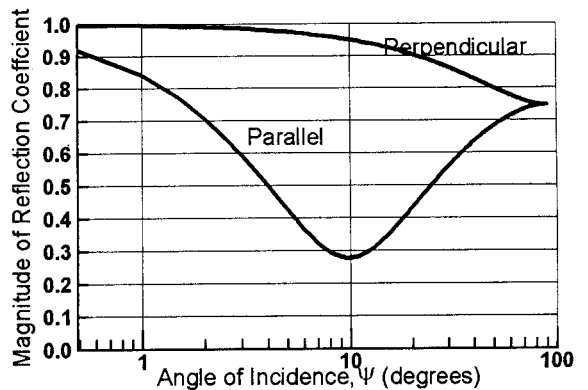
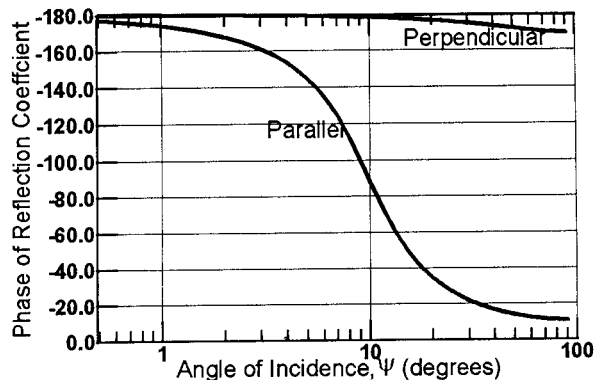
$$\delta = \frac{4\pi\Delta h}{\lambda} \sin \psi \quad (6)$$

where  $\Delta h$  is the standard deviation of the normal distribution for the surface roughness. The reflection geometry is shown in Figure 1.

Regarding polarization, the  $R_{\parallel}$  coefficient is for incident radiation in which the  $E$  field is oriented parallel to the plane of incidence, not the plane of the reflecting surface. Likewise,  $R_{\perp}$  is for  $E$  field polarization perpendicular to the plane of incidence. With vertical building wall reflections, for example, horizontal polarization is parallel to the plane of incidence while vertical polarization is perpendicular to the plane of incidence. Conversely, for horizontal ground surface reflections, horizontal polarization is perpendicular and vertical polarization is parallel. Some examples of the magnitude and phase of the reflection coefficient as a function of the angle of incidence  $\psi$  at 600 MHz are shown in Figures 2 and 3.

### C. DIFFRACTION

The energy diffracted from illuminated corners can be modeled using wedge diffraction coefficients, where the wedge has the physical characteristics of the corner. The

Figure 2: Magnitude of reflection coefficient.  $\sigma = 1.0$ ,  $\epsilon_r = 15$ , Frequency= 600 MHz.Figure 3: Phase of reflection coefficient.  $\sigma = 1.0$ ,  $\epsilon_r = 15$ , Frequency= 600 MHz.

complete solution for this canonical problem has been addressed in the uniform theory of diffraction (UTD) and reported initially in [9] for the perfectly conducting wedge case. For our propagation model, the wedges will have finite conductivity (typically the corners of stone surfaced buildings) so that the diffraction coefficients for finite conductivity wedges found in [10] are appropriate. Those diffraction coefficients are repeated here (with some changes in notation):

$$\begin{aligned} D_{\parallel}^{\pm} = & \frac{-e^{-j(\pi/4)}}{2n\sqrt{2\pi\beta}} \cdot \left[ \cot\left(\frac{\pi + (\phi - \phi')}{2n}\right) F(\beta La^+(\phi - \phi')) \right. \\ & + \cot\left(\frac{\pi - (\phi - \phi')}{2n}\right) F(\beta La^-(\phi - \phi')) \\ & + R_{\parallel,0}^{\pm} \cot\left(\frac{\pi - (\phi + \phi')}{2n}\right) F(\beta La^-(\phi + \phi')) \\ & \left. + R_{\parallel,n}^{\pm} \cot\left(\frac{\pi + (\phi + \phi')}{2n}\right) F(\beta La^+(\phi + \phi')) \right] \quad (7) \end{aligned}$$

where

$$F(x) = 2j\sqrt{x}e^{jx} \int_{\sqrt{x}}^{\infty} e^{-j\tau^2} d\tau \quad (8)$$

is a Fresnel integral, and

$$L = \frac{ss'}{s + s'} \quad (9)$$

is a distance term for the 2 dimensional case with  $s$  the distance from the observation point to the edge of the wedge and  $s'$  the distance from the illuminating source to the edge, and

$$a^\pm(\phi \pm \phi') = 2 \cos^2 \left( \frac{2n\pi N^\pm - (\phi \pm \phi')}{2} \right) \quad (10)$$

In (10),  $N^\pm$  are the integers which most closely satisfy the equations

$$2\pi n N^+ - (\phi \pm \phi') = \pi \quad (11)$$

$$2\pi n N^- - (\phi \pm \phi') = -\pi \quad (12)$$

The terms  $R_0$  and  $R_n$  refer to the reflection coefficients of the incident wedge face and opposite wedge face, as shown in Figure 4. They are computed using (2) and (3) for parallel and perpendicular polarization, respectively. Figure 5 shows an example of the magnitude of the diffraction field for a 90 degree wedge and an angle of incidence  $\phi'$  of 75 degrees.

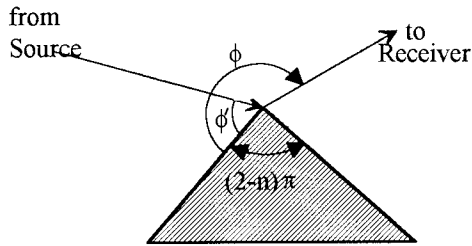


Figure 4: 2 dimensional wedge diffraction geometry.

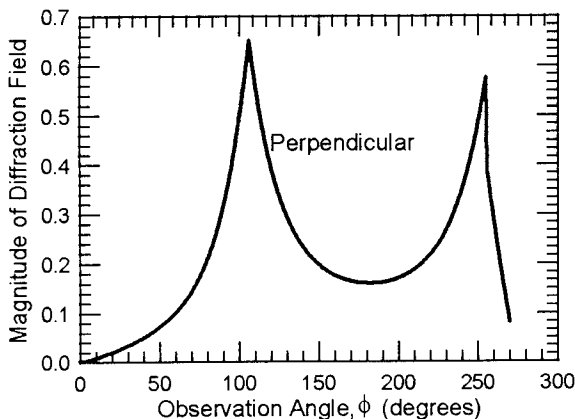


Figure 5: Magnitude of diffraction field.  $\phi' = 75^\circ$ ,  $\sigma = 1.0$ ,  $\epsilon_r = 15$ .

## D. DIFFUSE WALL SCATTERING

When the transmitted energy encounters a wall, that energy is either absorbed, transmitted through the wall, reflected (specular reflection), or scattered. In this model we are ignoring absorption. The specular reflection coefficient described above included a term which reduces the magnitude of the smooth surface specular reflection coefficient due to surface roughness. The energy not contained in the specular reflection from a rough surface is partly accounted for by scattered energy from the rough surface.

Scattering from rough or non-uniform surfaces and structures is the classic problem addressed by radar theory. The scattered energy is a function of the amount of energy illuminating the surface and the radar cross section (RCS) which in turn is a function of the illumination angle and the observation angle [11]. The RCS is usually denoted by  $\sigma^0$ , the normalized scattering coefficient for a square meter of illuminated surface. When multiplied by the total illuminated surface area, the total RCS,  $\sigma$ , for the scatterer is determined. The  $\sigma^0$  for various objects from various illumination angles is usually determined by measurement or calculation when the features of the structure are well known (and ray-tracing is sometimes used for these calculations). In the case of building walls, the particular roughness features are not well-known but may consist of window ledges and recesses, architectural and decorative features, and miscellaneous other appurtenances. No measurement data is available which indicates what the RCS should be, although knowing  $\Delta H$  for the surface can lead to a calculated estimate.

To compute scattered ray energy at the receiver, the power density on the wall is first computed and then multiplied by  $\sigma$  to yield the total scattered power from the surface. This scattered power is then attenuated by the usual geometric spreading as a function of  $1/d_s^2$ , where  $d_s$  is the distance from the scatterer to the receiver. When used in combination with the free space transmission formula in (2), the scattering coefficient becomes:

$$A_{scat} = \frac{\sigma}{4\pi d_s^2} \quad (13)$$

This scattering coefficient is used along with the other propagation primitives described above to find the scattered ray energy at the receiver.

## E. WALL TRANSMISSION

When a wall is illuminated with energy, some of it passes through the wall such that it can be received on the other side. The amplitude of this received energy is a function of the amplitude of the power illuminating the wall, and the amount of attenuation which occurs when the energy passes through the wall. A thick wall may have a very high transmission loss (essentially opaque), while glass walls may have only a fraction of a dB of attenuation.

Since no comprehensive data exists for the amount of wall transmission as a function of frequency which occurs with outside walls of the type and thickness commonly found in urban environments, the ray-tracing propagation model used here provides for a tabulated description of wall transmission as a function of frequency for each of the wall types in the propagation environment. This wall transmission coefficient is designated  $A_{tran}$ .

## F. RECEIVED RAY POWER

The five propagation primitives described are combined according to which features of the propagation environment a ray encounters in transit from the transmitter to the receiver. In general, the receiver ray power is given by:

$$P_r = \frac{P_t G_t G_r \lambda^2}{(4\pi)^2 d^2} \left[ \prod_j R_j \right]^2 \left[ \prod_k A_k(s', s) D_k \right]^2 \quad (14)$$

where the first term is just the free space component from (2),  $R_j$  is the reflection coefficient from (3) or (4) for the  $j^{th}$  path reflection, and  $D_k$  is the diffraction coefficient from (7) for the  $k^{th}$  path diffracting wedge. The diffraction coefficients are also multiplied by a special spatial attenuation function  $A_k(s', s)$  which finds the correct multiplicative diffraction coefficient given the  $1/d^2$  dependence in the first term in (14). Although this equation is for the received power, in the propagation model all rays are handled as complex voltage values which are affected by the complex reflection and diffraction coefficients. By this means the magnitude and phase of each ray for both HP and VP transmissions are computed at the receiver.

If there is a scattering interaction on the ray path,  $P_r$  in (14) is multiplied by  $A_{scat}$  in (13), a scalar. Similarly, if wall transmission is involved on the path,  $P_r$  in (14) is multiplied by  $A_{tran}$ .

In the ray-tracing model used here, scattered rays and wall-transmitted rays are not onward-propagated. That is, scattered and wall-transmitted rays cannot illuminate other walls or corner wedges, nor induce new scattering or wall transmission. Scattering or wall transmitted energy is thus at the end of the line; it can only illuminate the receiver.

## III. TRANSMISSION CHANNEL CHARACTERISTICS

At each receive location the ray-tracing propagation model provides three types of information about the transmission channel:

1. Mean signal level (mean channel path loss from the transmitter to the receiver)
2. RMS delay spread and the specific impulse response as shown in (1)

3. An estimate of the flat fading envelope amplitude distribution

### A. MEAN SIGNAL LEVEL

The mean signal level is found by simply averaging the total power in the rays arriving at the receiver. Fade depth statistics are considered relative to this mean.

### B. RMS DELAY SPREAD

The RMS delay spread is the second central moment of the power delay profile with the first arriving ray  $\tau_{min}$  referenced as  $t = 0$ , and other arrival delay times  $\tau_n$  found relative to  $\tau_{min}$ . The RMS delay spread is then calculated:

$$\sigma_\tau = \left[ \sum_{n=1}^N (\tau_n - \bar{\tau})^2 p(\tau_n) \right]^{\frac{1}{2}} \quad (15)$$

where the mean value of the power delay profile is

$$\bar{\tau} = \sum_{n=1}^N (\tau_n) p(\tau_n) \quad (16)$$

and

$$p(\tau_n) = \frac{A_n^2}{\sum_{n=1}^N A_n^2} \quad (17)$$

### C. FLAT FADING STATISTICS

The third channel characteristic which the propagation model provides is an estimate of the probability density function (pdf) for the spatially-dependent flat fading envelope amplitude at the receive location. In this case, "flat fading envelope" refers to the envelope of the signal over a sufficiently narrow bandwidth that frequency-selective (or wideband) fading is not considered. Hence flat fading is sometimes referred to as "narrowband" fading. Usually this fading pdf is taken as Rayleigh distributed. However, in many receiver locations, especially those which are line-of-sight, the fading pdf is more closely represented by a Rice distribution. The ray-tracing propagation model provides a means of estimating the actual pdf at a receive location. This is done by supposing that the receiver moves over a range of  $\pm 5\lambda$  or  $\pm 10\lambda$ . The amplitude of the envelope is then computed every  $1/8\lambda$  by the vector addition of all the rays and considering the path length-dependent phase shift and arrival angle of each ray. This set of values is then a sample set from the actual flat fading envelope voltage  $r$  which is a continuous random variable, and stationary at least in the immediate vicinity of receive point. Estimates of the mean  $\hat{r}$  and variance  $\hat{\sigma}_r^2$  of the envelope pdf can be found from the  $K$  sample points.

$$\hat{r} = \frac{1}{K} \sum_{k=1}^K r_k \quad (18)$$

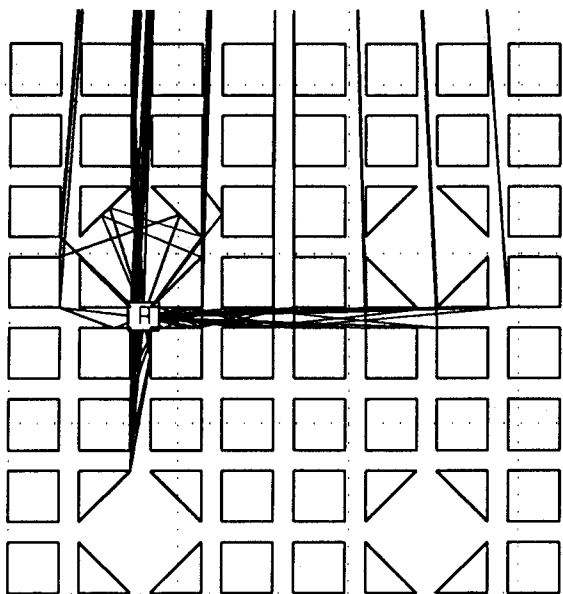


Figure 6: Hypothetical urban city plan. Block size = 75 X 75 meters, street width= 30 meters.

$$\widehat{\sigma}_r^2 = \frac{1}{K-1} \sum_{k=1}^K (r_k - \widehat{r})^2 \quad (19)$$

The general Rice distribution used to represent the envelope amplitude fading distribution is

$$p(r) = \frac{r}{\sigma_r^2} \exp\left(\frac{-r^2}{2\sigma_r^2}\right) \exp\left(\frac{-A_c^2}{2\sigma_r^2}\right) I_0\left(\frac{rA_c}{\sigma_r^2}\right) \quad (20)$$

where  $A_c$  is taken here as the highest amplitude ray in the power delay profile and  $I_0$  is the modified Bessel function of the first kind. When  $A_c$  is small compared to  $\sigma_r$ , the distribution  $p(r)$  is essentially Rayleigh and the fading depth probability follows the well known Rayleigh distribution. When the delay profile is dominated by a single strong ray, and  $\sigma_r$  is small compared to  $A_c$ , the fading envelope distribution is more closely confined around the amplitude of  $A_c$ , resulting in less probable fades of a given depth.

The degree of Ricean-like characteristics of the envelope amplitude pdf are sometimes indicated by the following factor:

$$k = 10 \log\left(\frac{A_c^2}{2\sigma_r^2}\right) \quad (21)$$

Low and negative values of  $k$  indicate a more Rayleigh-like fading distribution; higher values of  $k$  indicated a more Ricean-like pdf.

#### IV. PROPAGATION STUDIES IN AN URBAN ENVIRONMENT

The propagation model described above was used with the hypothetical city plan shown in Figure 6. The city

plan occupies about one square kilometer with a block size of 75 meters and street widths of 30 meters which correspond to a typical dense downtown urban area. In this example, the wall conductivities were set at 1.0 S/m with relative permittivities of 15. The walls were all considered to be much higher than the elevation of the rays as they interacted with the walls; therefore, a 2 dimensional model can appropriately handle this situation.

For the studies done here, the transmitter was placed at a location 5 km north of the city area with an omnidirectional ERP of 100 kW for both horizontal and vertical polarizations. Although the actual transmitter distances from a city may vary widely, the absolute distance of the transmitter from the reception environment only sets absolute delay, not the relative delays between multipath echos which are of interest here. Such time delays are primarily a function of building locations and street widths. Also, because of the limited area considered here, long delayed echos from distant buildings, towers, or mountains are not considered. As noted in the introduction, HDTV systems are equipped with equalizers which are designed to handle such static isolated long delay echos. This study example is designed to illustrate the multitude of closely spaced multipath echos with relative time delays on the order of the inverse of the channel symbol rate which may not be static, but which the equalizer must effectively treat. Hence, the limited area model environment shown in Figure 6 provides useful information about the channel response for HDTV and other digital broadcast systems. The receive antenna was assumed to be omnidirectional for the results shown in Figures 7, 8, 9, and 10.

Figure 6 also shows the rays from the transmitter as they are reflected and diffracting off the walls and corners on their way to the receiver shown by an "R". The amplitude and phase of these rays at the receiver form the channel impulse response.

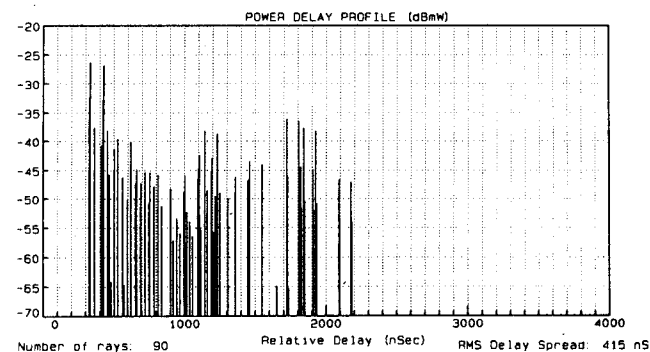


Figure 7: HP power delay profile for point R in Figure 6.

#### A. POWER DELAY PROFILES

Figure 7 shows a typical power delay profile for the HP signal at the receive location in Figure 6. This is the basic channel impulse response as formulated in (1) where the amplitude and phase of each of the  $N$  rays are found from

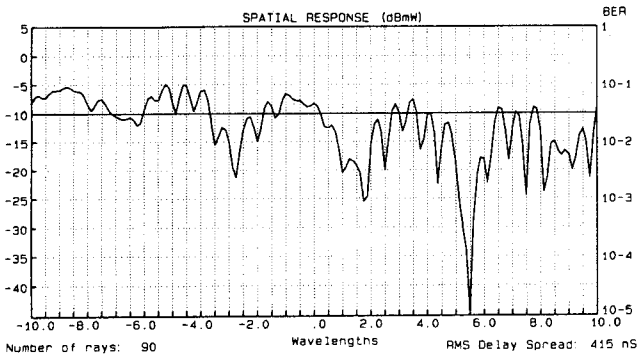


Figure 8: Flat fading envelope for HP at point R.

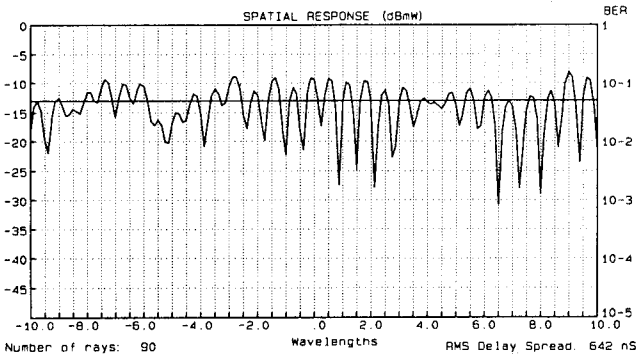


Figure 9: Flat fading envelope for VP at point R.

the ray-tracing propagation model. The information in the power delay profile is fundamental to determining the inter-symbol interference (ISI), and thus error rate, in a wideband digital system.

## B. CORRELATION OF HP AND VP SIGNAL ENVELOPES

Figures 8 and 9 show the flat (narrowband) fading envelopes for the HP and VP signals, respectively, at point R. The fading waveforms in Figures 8 and 9 are actually samples of the fading waveform for HP and VP with samples taken every  $\lambda/8$ . By sampling over a sufficiently long distance ( $\pm 10\lambda$  in the case) it is possible to calculate the linear correlation coefficient,  $\rho_l$ , for this sample of 160 data points using the following formula:

$$\rho_l = \frac{\sum_n (h_n - \bar{h})(v_n - \bar{v})}{N \sqrt{\sigma_h^2 \sigma_v^2}} \quad (22)$$

where  $\bar{h}$  and  $\bar{v}$  are the mean values of the HP and VP voltage envelopes, respectively, and  $\sigma_h^2$  and  $\sigma_v^2$  are the corresponding variances of the envelope waveform, both estimated from the  $N$  waveform samples as shown in (18) and (19).

The linear correlation coefficient is a simple measure of the degree of association between two variables but otherwise is a weak statistical parameter since it carries no information about the shape of the pdf's involved. Therefore, it is difficult to test the statistical significance of the resulting value of  $\rho_l$ . Nonetheless, it will suit the purpose

here of assessing the degree of correlation between the HP and VP signal envelopes.

The correlation coefficient between the HP and VP envelope waveforms was calculated at a series of points along a route which followed along one of the streets in the grid shown in Figure 6 for approximately 250 meters, turned a corner, and continued down a second street for about 250 meters. Points were spaced every five meters.

At each point along the route the correlation coefficient was computed as described above. The results are shown in Figure 10. The plot shows that the correlation coefficient is generally in the range of  $\pm 0.3$ , with occasional spikes outside this range. This significant lack of correlation is an indication that the use of HP/VP polarization diversity switching might be useful for improving the integrity of HDTV reception.

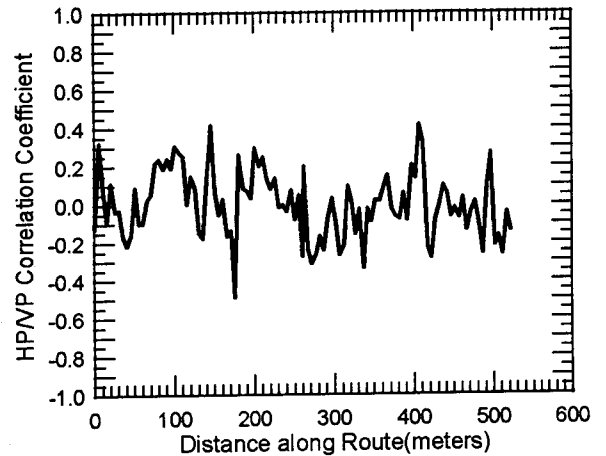


Figure 10: HP/VP flat fading envelope correlation coefficient along the test route.

## C. URBAN AREA CHANNEL RESPONSE

The information given above illustrates the type of data which can be developed from the ray-tracing propagation model. For a comprehensive study of urban propagation, the model was used to analyze the channel characteristics at a grid of points along the streets in the hypothetical city plan. To simulate a more realistic reception scenario, the studies were done with both an omnidirectional receive antenna and a 9 dBd gain Yagi receive antenna. The computer program which implements the ray-tracing allows for the receive antenna to automatically be pointed in the direction of the maximum amplitude ray, which would normally (though not always) be the antenna installation choice. The cumulative distribution results for HP, VP and circular polarization (CP) for the RMS delay spread are shown in Table 1 for the omni-directional receive antenna and in Table 2 for the optimally-oriented Yagi antenna.

Table 1 shows that an RMS delay spread of about 340 to 350 nSec or more is found at 50% of the locations for HP,

VP and CP, although the spread of the VP distribution is larger than that for HP or CP. Given the particular reflection characteristics of one polarization versus the other, it is not surprising that the distributions are different in this way.

Table 2 shows the expected substantial reduction in RMS delay spread with the Yagi receive antenna. This Table also shows that CP offers a distinct reduction in RMS delay spread when compared to HP or VP only. As Figures 2 and 3 show, for certain angles of incidence, upon reflection the parallel-polarized signal undergoes an almost 180° phase shift relative to the perpendicular polarization. The 90° phase shifts built into the CP transmit and receive antennas for one polarization, in combination with the reflection phase shift, can result in substantial cancellation of an odd-order reflection signal at the receive antenna terminals. Cancellation of the reflected signal is not complete, of course, because after reflection the relative magnitudes of the two polarizations also change such that the signal is elliptically-polarized. Regardless of its rotational sense, an EP signal with unequal major and minor amplitude axes cannot be completely rejected by a CP receive antenna.

% of locations	Delay spread is less than:		
	HP	VP	CP
1.0	43.2	31.0	41.8
5.0	52.5	35.0	50.0
10.0	58.9	40.1	57.2
25.0	168.1	194.6	165.2
50.0	342.4	351.0	337.2
75.0	552.5	581.4	514.9
90.0	801.9	958.3	699.0
95.0	801.9	958.3	803.2
99.0	801.9	958.3	803.2

Table 1: Cumulative distribution of RMS delay spread in nSec using omni-directional receive antenna.

% of locations	Delay spread is less than:		
	HP	VP	CP
1.0	41.6	30.6	40.7
5.0	48.2	33.1	44.4
10.0	52.1	36.2	49.0
25.0	61.1	55.3	59.5
50.0	154.4	172.6	126.7
75.0	358.0	327.6	293.5
90.0	554.4	520.0	483.8
95.0	727.5	760.0	578.3
99.0	727.5	760.0	830.0

Table 2: Cumulative distribution of RMS delay spread in nSec using 9 dBd gain Yagi receive antenna.

## V. CONCLUSIONS

A ray-tracing propagation model has been presented which can account for the multitude of reflecting, diffracting and scattering sources in an urban area. The model predicts several channel response characteristics at specific receive locations, including mean path loss, RMS delay spread, and flat fading envelope amplitude distribution statistics.

A propagation study in a hypothetical urban environment showed that 50% of the locations had RMS delay spreads of about 154 and 172 nSec for HP and VP, respectively, and 126 nSec for CP when using a Yagi receive antenna oriented toward the maximum received signal ray. This is an interesting indication that CP might be better suited for HDTV transmission in urban areas than either HP or VP alone.

With RMS delay spread values ranging to several hundred nanoseconds in urban areas, a 20 Mbit 16QAM HDTV system would be hopelessly unworkable without a very effective adaptive equalizer. Besides the equalizer, a directional receive antenna which suppresses some multipath signals in favor of others, and circular polarization, appear to be useful techniques to increase overall system process gain and thereby improve bit error rate performance.

## ACKNOWLEDGEMENT

The author wishes to thank Andy R. Nix of the Centre for Communications Research at the University of Bristol for discussions and comments which were helpful in the preparation of this paper.

## REFERENCES

- [1] G.L. Turin et.al. "A statistical model for urban multipath propagation," *IEEE Trans. Veh. Technol.*, vol. VT-21, pp. 1-9, Feb. 1972.
- [2] W.L. Stutzman and G.L. Thiele, *Antenna Theory and Design*. New York: John Wiley & Sons, 1981, p. 447.
- [3] K.J. Gladstone and J.P. McGeehan, "Computer simulation of multipath fading in the land mobile radio environment," *IEE Proc.*, vol. 27, Pt. G, pp. 323-330, no. 6, Dec. 1980.
- [4] J.W. McKown and R.L. Hamilton. "Ray-tracing as a design tool for radio networks," *IEEE Networks Mag.*, pp. 21-26, Nov. 1991.
- [5] K.S. Schaubach, N.J. Davis, and T.S. Rappaport, "A ray-tracing method for predicting path loss and delay spread in microcell environments," *Proceedings of the 1992 IEEE Veh. Tech. Society Conf.*, Denver, pp. 932-935, May 1992.

- [6] M.C. Lawton and J.P. McGeehan. "The application of GTD and ray launching techniques to channel modelling for cordless radio systems," *Proceedings of the 1992 IEEE Veh. Tech. Society Conf.*, Denver, pp. 125-130, May 1992.
- [7] W.L. Stutzman and G.L. Thiele, *Antenna Theory and Design*. New York: John Wiley & Sons, 1981, p. 61.
- [8] K.A. Chamberlain and R.J. Leubbers. "An evaluation of Longley-Rice and GTD propagation models," *IEEE Trans. Antennas Propagat.*, vol. AP-30, no. 6, pp. 1093-1098, Nov. 1982.
- [9] R.G. Kouyoumjian and P.H. Pathak, "A uniform geometric theory of diffraction for an edge on a perfectly conducting surface," *Proc. IEEE*, vol. 62, no. 11, pp. 1448-1461, Nov. 1974.
- [10] R.J. Leubbers, "Finite conductivity uniform GTD versus knife edge diffraction in prediction of propagation path loss," *IEEE Trans. Antennas Propagat.*, vol. AP-32, no. 1, pp. 70-76, Jan. 1984.
- [11] J.L. Eaves and E.K. Reedy, *Principles of Modern Radar*. New York: Van Nostrand Reinhold Company, 1987, pp 9-11.